Article

Synthesis and characterization of ionic liquids by imidazolium salts derivatives and study Molecular docking of compounds

Shaymaa A. Mohammed

Chemistry department, Faculty of Science, University of Al- Muthana, Samawa, Iraq.

A. lecturer Email: shiemaa@mu.edu.iq

Abstract:

Ionic liquids represent a new category of compounds that have attracted considerable interest in current research. Derived from traditional concepts, these substances have shown impressive performance across various applications. The synthesis involves mixing new alkyl halides with a specific class of compounds, namely methyl and benzyl imidazole, to create the desired ionic liquids. Characterization of these newly synthesized compounds is carried out using techniques such as ^1H NMR, FT-IR, and UV-Visible spectroscopy.

Keywords: Ionic liquids, imidazole

Introduction

“Ionic liquids have unique properties that distinguish them from conventional materials. Often referred to as salts, these compounds exhibit a distinct structure characterized by a high ionic character and the presence of inorganic or elemental counter ions with negative charges.” Notably, ionic liquids can be classified as low-melting materials, with melting points below 100 degrees Celsius. “Their low vapor pressure, high viscosity, substantial density, non-flammability, and compatibility with

both organic solvents and water make ionic liquids increasingly popular as environmentally friendly alternatives in various chemical processes."

Moreover, the regulations regarding ancient civilization liquids have resulted in numerous requests that hinder the extraction of specific components, including advanced microscopic materials, catalysts, and odorless vapors, as well as outcomes related to lithium processes. Within the scope of civil service, both academic and industrial research face significant challenges in finding environmentally safe yet cost-effective alternatives, particularly concerning traditional liquid types like 1,3-dialkylimidazolium and benzimidazolium cations, which have gained considerable attention from numerous research groups in recent decades. The 1-alkyl-3-methylimidazolium derived from traditional fluids has displayed a diverse range of stable compounds, serving as an effective medium for isolating non-toxic substances due to the unique characteristics of these materials.

Experimental part

Analytical Procedures: FT-IR spectra were recorded using a Fourier transform infrared spectrophotometer, specifically the Shimadzu FT-IR-8400S, with KBr plates for sample preparation at the University of Kufa. "UV-visible spectra were obtained using a double beam Shimadzu UV 1650 PC spectrophotometer, with analyses conducted based on the local expertise at the University of Kufa. Thin-layer chromatography was performed on Merck F-256 silica gel plates using various suitable eluents. The ^1H NMR spectra were recorded using a Bruker Fourier transform spectrometer operating at 400 MHz, with D2O as the solvent." Analyses took place at the University of Mashhad, focusing on parameters such as allure, strength of education, and institutional affiliation.

2-2 Synthesis Process: In the synthesis, a mixture of 2-bromo-N-(4-nitrophenyl)-acetamide and 4-nitroaniline (2.13 g, 0.0154 mol) was dissolved in 15 ml of a suitable solvent, and 6 ml of pyridine was added. The mixture was stirred for 30 minutes at 0°C, after which 3.5 g (0.0173 mol) of bromoacetyl bromide was introduced dropwise. The resulting mixture was stirred for 24 hours at room temperature. After this duration, the reaction was quenched with 50 ml of water, and the organic layer was separated. The aqueous phase was dried over sodium sulfate, filtered, and the solvent was evaporated, yielding a dark viscous residue weighing 2.5 g (85% yield).

Synthesis of the Desired Compound: For the synthesis of the target compound, Compound 3 was dissolved in 25 ml of acetonitrile and stirred to achieve homogeneity. Methyl or benzyl imidazole (2) (0.0126 mol) was then added to the solution. The mixture was heated to 50°C for 24 hours with continuous stirring. Following this, the acetonitrile was removed under reduced pressure to obtain the desired product in concentrated yield.

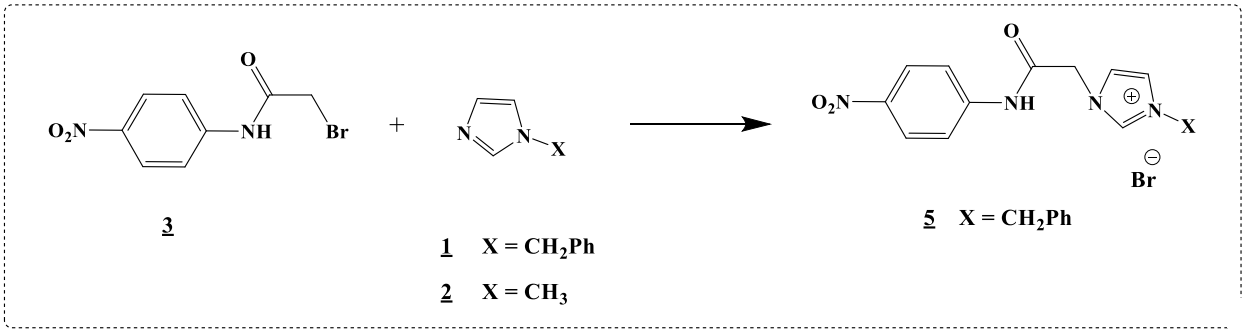

3

1 X = CH_2Ph

2 X = CH_3

5 X = CH_2Ph

1- The compound 2-3-1,benzyl-3-(2-((4-nitrophenyl)amino)-2-oxoethyl)imidazol-3-ium bromide, was synthesized by reacting Compound 3 (3 g, 0.0115 mol) with benzylimidazole 1 (1.83 g, 0.0115 mol) according to the comprehensive procedure described in (2-3). The reaction yielded a total of 3.9 g of the product, which corresponds to a 76% yield. The ^1H NMR spectrum (400 MHz, Deuterated Solvent)

exhibited the following chemical shifts: δ 8.76 (s, 1H), 8.43 (d, J = 7.1 Hz, 1H), 7.93 (d, J = 7.1 Hz, 1H), 7.40 – 7.12 (d, J = 8.4 Hz, 2H), 6.97 (d, J = 8.4 Hz, 2H), 5.64 (s, 2H), and 5.01 (s, 3H).

2. The compound 2-3-2,methyl-3-(2-((4-nitrophenyl)amino)-2-oxoethyl)imidazol-3-ium bromide, was synthesized from Compound 3 (3 g, 0.0115 mol) and methylimidazole 2 (0.95 g, 0.011 mol) following the established procedure described in (2-3). This reaction produced a product yield of 0.72 g, resulting in a 75% yield.

3. **Results and Discussion:** The synthesis of the compounds was performed using a well-defined and reproducible approach, as demonstrated in Scheme 2.

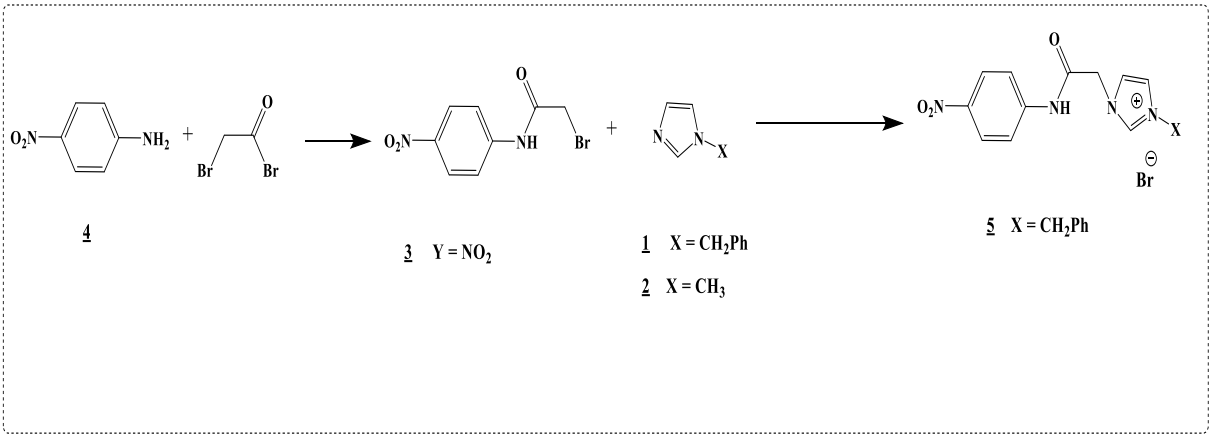

Scheme (2) : Synthesis of compound 5

The process began with the reaction of an aniline derivative with bromoacetyl bromide, using pyridine as a catalyst to promote the formation of hydrochloric acid as a byproduct. This reaction occurred rapidly, resulting in a moderate yield of product. Nonetheless, the resulting compound was deemed suitable for further processing beyond the initial synthesis. “The infrared spectrum of compound 3 revealed characteristic peaks, including 3263 cm^-1 corresponding to the NH group of the amide, 3128 cm^-1 associated with aromatic C-H stretching, and a peak at 1672 cm^-1 related to C=O stretching vibrations. Additionally, peaks within the

range of 1600-1480 cm^-1 were likely due to aromatic C=C stretching. A peak at 1186 cm^-1 was identified as C-O stretching. Moreover, compound 3 displayed distinct peaks at 1571 and 1344 cm^-1, which likely indicated the presence of a nitro (NO2) group (Figure 1).”

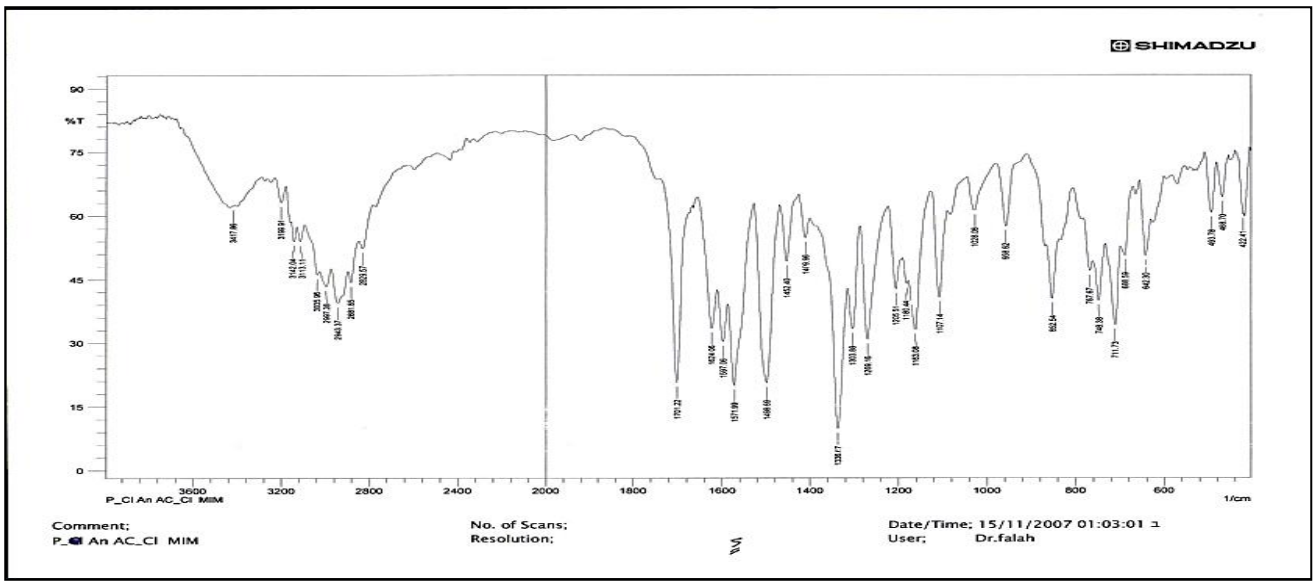

Fig (1): FT-IR range of compound **3**

“Compounds 5 were successfully synthesized from compound 3 through reactions with either benzyl imidazole 1 or methyl imidazole 2 in acetonitrile at equimolar ratios.” The chloride group’s proximity to the carbonyl in compound 3 rendered it reactive, facilitating the transformation into the desired products with a high level of reliability, as indicated by the melting point data. The reaction mechanism followed an SN2 pathway, in which the electron pair from the nitrogen group attacked the methylene carbonyl of compound 3, leading to the displacement of the chloride group and the formation of a positively charged cation (Scheme 3). FTIR analysis (Figures 2 and 3) displayed distinct peaks corresponding to specific functional groups, which are summarized in Table 1.

Table 1: FTIR peaks of compounds 5

Compound	N-H	C-H ar	C-H al.	C=O	C=N	C=C	NO_2	C-H
5	3431	3059	2918	1695	1618	1560, 1494	1500,1344	1369, 1286

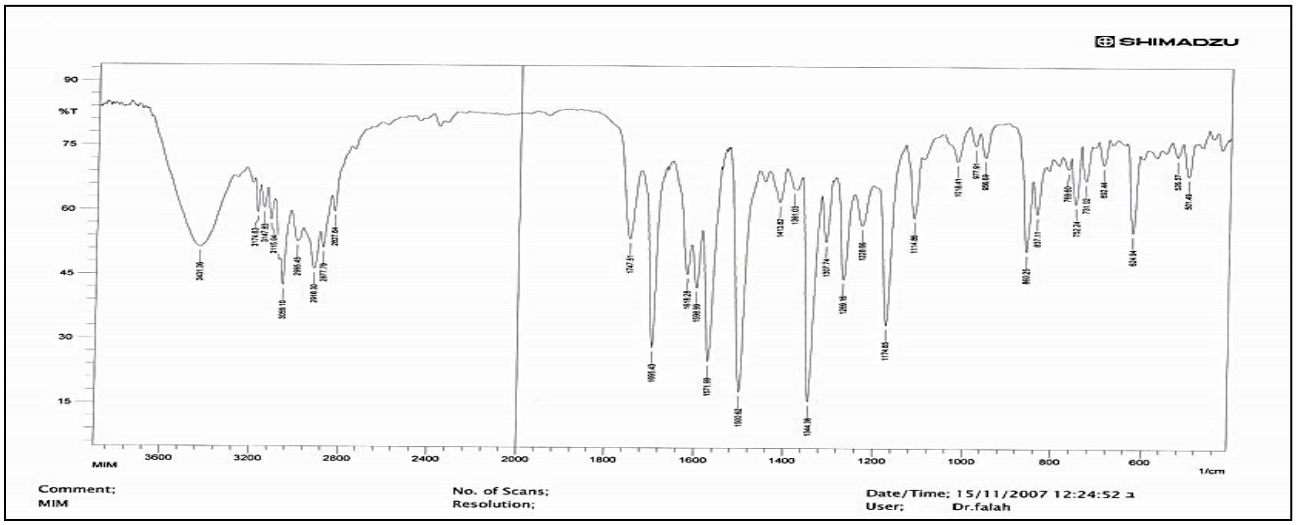

Fig (2) : FT-IR range of compound **5**

Compounds 5 were successfully synthesized from compound 3 by reacting it with either benzyl imidazole 1 or methyl imidazole 2 in acetonitrile at equimolar ratios. The reactivity of compound 3 was attributed to the positioning of the chloride group next to the carbonyl, which facilitated the reaction and ensured a complete transformation into the desired products with a high level of reliability, as shown by the melting point data. The reaction mechanism followed an SN2 pathway, in which the electron pair from the nitrogen group attacked the methylene carbonyl of compound 3, resulting in the displacement of the chloride group and the formation of a positively charged cation (Scheme 3). FTIR analysis (Figures 2 and 3) displayed distinct peaks that corresponded to specific functional groups, summarized in Table 1.

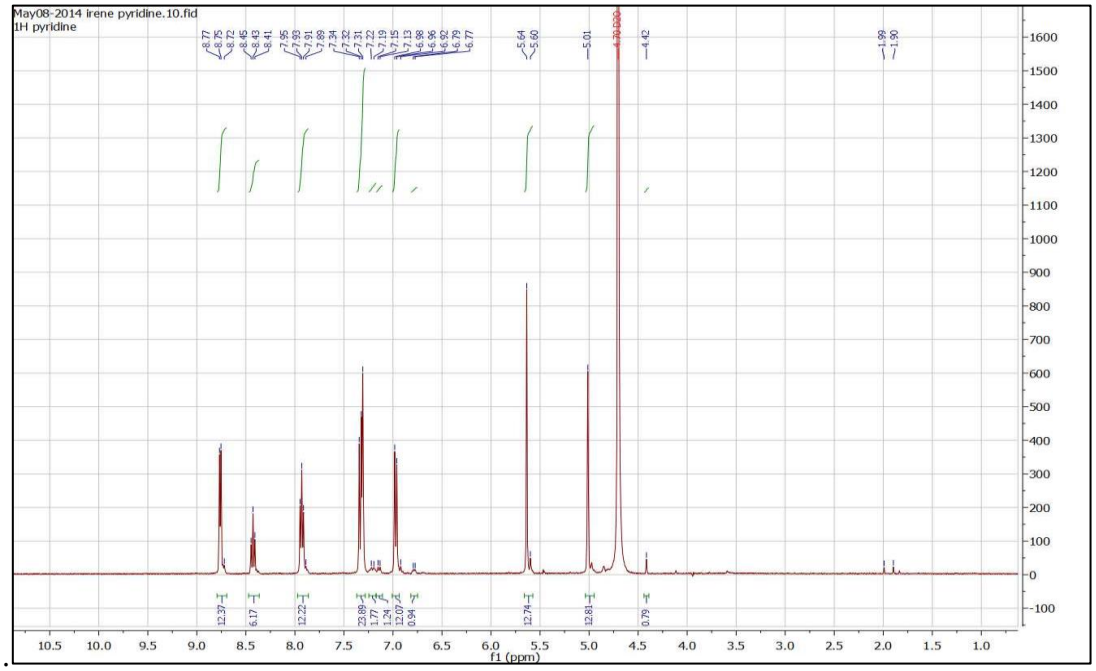

Fig (3-5): The IR spectrum of compound **5**

Molecular docking analysis of compounds targeted against the Klebsiella pneumoniae protein: Performance comparison with Imipenem

Molecular docking results for the Klebsiella pneumoniae protein using two different compounds were analysed and compared to Imipenem reference data. The reference data showed binding energy values ranging from -6.3410 to -5.2659, providing a benchmark for comparison.

(S)	RMSD
-6.2410	1.6782
-5.3027	2.5246
-5.2350	2.0647
-5.1720	1.3191
-5.1659	0.3515

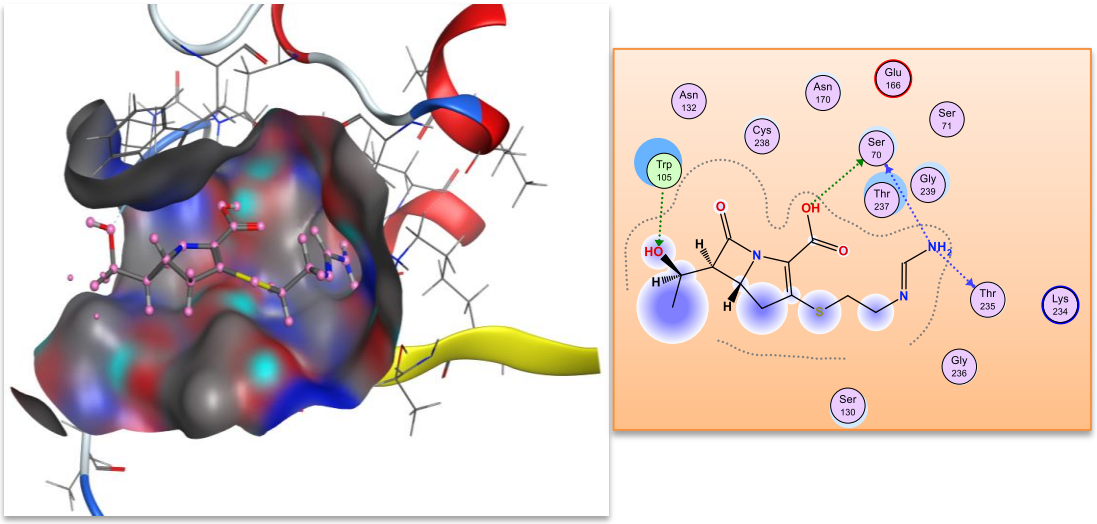

Figure 1 :Molecular interaction analysis and visualisation of protein active sites with binding energy and root deviation values

As for compound I, it showed the best binding energy of -6.73474, reflecting strong binding to the target protein. Compound I also achieved other binding values such as -6.68489 and -6.53177, further enhancing its performance compared to Imipenem. The second compound came with a better correlation value of -6.22365, with other values such as -6.12498 and -6.01616, showing an acceptable efficacy but was less efficient than the first compound **Table 1**.

When comparing the performance of the two compounds with the Imipenem reference data, it is clear that both compounds showed superior performance to the

reference. **Compound 1** showed clear superiority with correlation energy values of **-6.73474,** which is significantly lower than the minimum values of the reference. The second compound performed well with a better value of **-6.22365**, but did not reach the efficiency of the first compound.

Table 1. results Imipenem with receptor 8TN0

mol	S	rmsd_refine
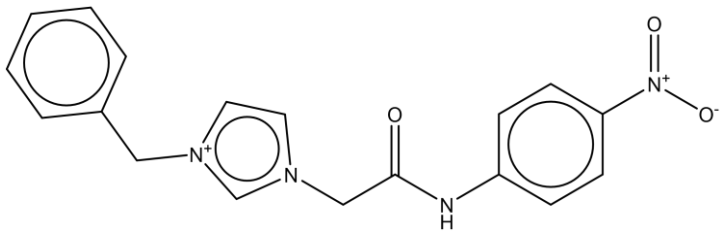	-6.73474	1.4110154
	-6.68489	2.1136522
	-6.53177	1.1291498
	-6.49293	1.1134255
	-6.48373	3.4056449
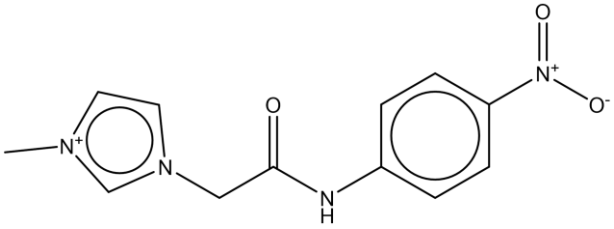	-6.22365	1.0305244
	-6.12498	1.0266736
	-6.01616	3.6390889
	-5.81475	1.4105306
	-5.75637	1.2051672

When comparing the performance of the two composites with the reference data, it is clear that both composites showed superior performance to the reference. **Compound 1** showed a clear superiority with a correlation energy value of -6.73474, which is significantly lower than the minimum value of the reference. The second composite performed well with a better value of -6.22365, but did not reach the efficiency of the first composite.

This reflects the ability of the first compound to achieve stronger and more stable binding to the protein, as the values showed remarkable stability in interacting with the active site of the protein. For the second compound, its good performance indicates that it can be considered as a viable second candidate. The stability of the

results enhances the reliability of the data, as molecular dynamics simulations showed the stability of the two compounds during the binding process.

Based on this analysis, Compound I can be considered as a promising candidate with its high binding energies of -6.73474 and superior performance in most values, while Compound II shows good performance but less efficient compared to Compound I. Future experimental studies including molecular dynamics simulations and in vitro tests are recommended to confirm the biological activity of the two compounds against Klebsiella pneumoniae and reinforce the results of this study.

Analysing the molecular docking of the two compounds with the Klebsiella pneumoniae protein reveals interesting details about the interactions occurring within the active site. Compound 1 showed a remarkable ability to interact effectively with the target protein, forming strong hydrogen bonds with amino acids Thr237 and Gly239, which helped to stabilise it within the active site. The presence of electrostatic interactions with residues such as Asp131 further stabilised the compound. Besides, amino acid residues such as Ser130 and Cys238 play an important role in creating a stable environment that supports the binding of the compound. Moreover, hydrophobic interactions with Trp105 and Tyr129 highlight the dynamic nature of this interaction, enhancing the efficacy of compound I and making it a promising candidate for inhibiting the activity of the target protein **Figure 2,Table2**.

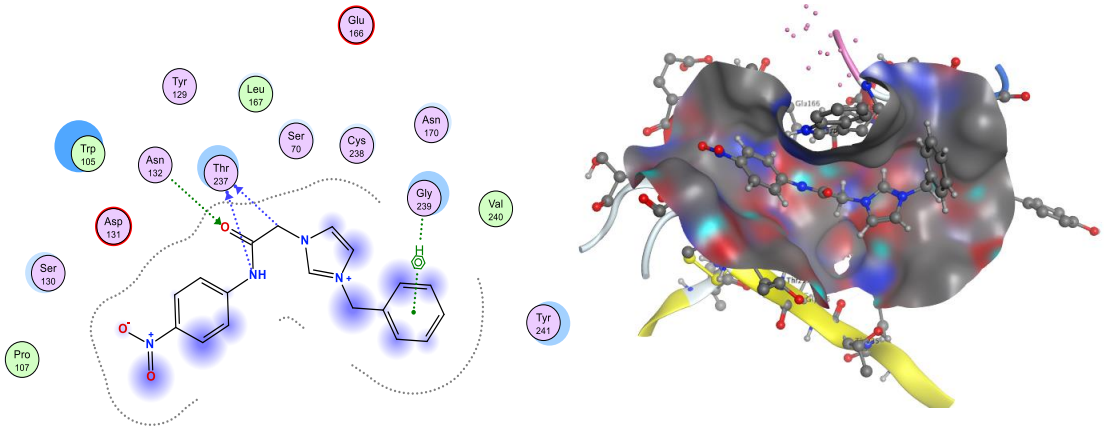

Figure 2: Compound 1 interconnection with the receptor 8TN0

As for the second compound, it also showed remarkable interactions with the active site of the protein, forming hydrogen bonds with amino acids Thr237 and Ser70, indicating its good stability. The interaction with Glu291 added a positive aspect reflecting the compound's ability to interact with the surface charge of the active site. Other amino acids such as Arg220 were effective in supporting electrostatic interactions, while Gly239 and Thr235 contributed to maintaining the optimal positioning of the compound within the active site. Although the second compound showed good performance, the strength and number of interactions were lower compared to the first compound, making it relatively less efficient **Figure 3, Table2**..

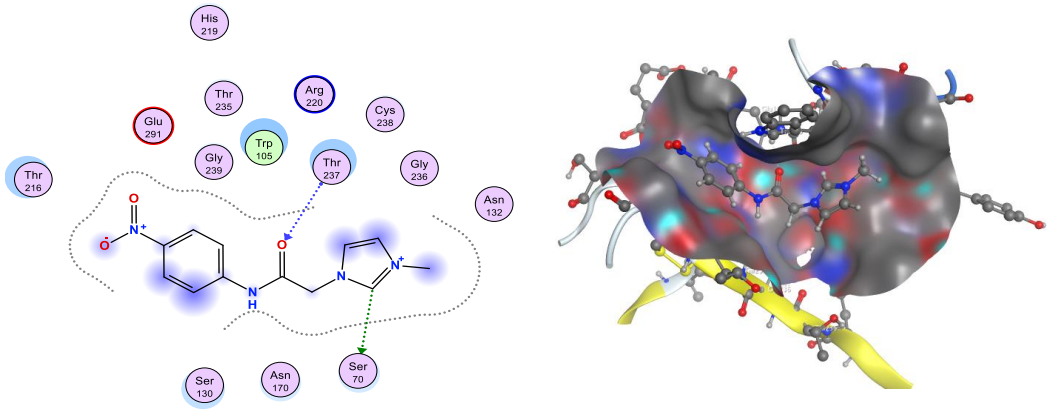

Figure3 : Compound 2 interconnection with the receptor 8TN0

Table 2. Analyses interactions between Compound 1 and 2 with receptor 8TN0

Compound 1				
Ligand	**Receptor**	**Interaction**	**Distance (Å)**	**E (kcal/mol)**
N7	11	H-donor	3.09	-0.9
C9	14	H-donor	3.38	-0.8
O11	18	H-acceptor	3.31	-1.8
6-ring	CA	pi-H	3.77	-0.9
Compound 2				
C12	19	H-donor	3.40	-0.5
O11	18	H-acceptor	3.35	-1.0

References

1- Lei, Z., Chen, B., Koo, Y.-M., & MacFarlane, D. R. (2017). *Introduction: Ionic Liquids. Chemical Reviews, 117(10), 6633–6635.* doi:10.1021/acs.chemrev.7b00246

2- Das, S., Kashyap, N., Kalita, S., Bora, D. B., & Borah, R. (2020). *A brief insight into the physicochemical properties of room-temperature acidic ionic liquids and their catalytic applications in C C bond formation reactions. Advances in Physical Organic Chemistry, 1–98.* doi:10.1016/bs.apoc.2020.07.002.

3- Huang, T.-Y., Ho, J. S., Goh, S., & Chong, T. H. (2021). *Ethanol recovery from dilute aqueous solution by perstraction using supported ionic liquid membrane (SILM). Journal of Cleaner Production, 298, 126811.* doi:10.1016/j.jclepro.2021.126811.

4- Senthil, K., Anand, S., & Kalainathan, S. (2020). *The Effect of Molecular Structure on Second-order Nonlinear Optical Properties of Stilbazolium*

Derivative Single Crystals: A review. Journal of Materials Chemistry C. doi:10.1039/d0tc04260a.

5- Hussin, F., & Aroua, M. K. (2020). Recent trends in the development of adsorption technologies for carbon dioxide capture: A brief literature and patent reviews (2014–2018). Journal of Cleaner Production, 253, 119707. doi:10.1016/j.jclepro.2019.119707.

6- Yang, G., Jiao, Y., Yan, H., Tian, C., & Fu, H. (2021). *Electronic Structure Modulation of Non-Noble-Metal-Based Catalysts for Biomass Electrooxidation Reactions. Small Structures, 2100095*. doi:10.1002/sstr.202100095.

7- Z. Chen, J. H. Pereira, H. Liu, H. M. Tran, N. S. Y. Hsu, D. Dibble, S. Singh, P. D. Adams, R. Sapra, M. Z. Hadi, B. A. Simmons, and K. L. Sale, "Improved activity of a thermophilic cellulase, Cel5A, from Thermotoga maritima on ionic liquid pretreated switchgrass," *PLoS One*, vol. 8, no. 11, pp. 1–9, 2013.

8- Singh, S. K., & Savoy, A. W. (2019). *Ionic liquids synthesis and applications: An overview. Journal of Molecular Liquids, 112038.* doi:10.1016/j.molliq.2019.112038.

9- S. Gallagher, L. Florea, K. J. Fraser, and D. Diamond, "Swelling and shrinking properties of thermo-responsive polymeric ionic liquid hydrogels with embedded linear pNIPAAM," *Int. J. Mol. Sci.*, vol. 15, no. 4, pp. 5337–5349, 2014.

10- Sanchora, P., Pandey, D. K., Kagdada, H. L., Materny, A., & Singh, D. K. (2020). *Impact of Alkyl Chain Length and Water on the Structure and Properties of 1-alkyl-3-methylimidazolium Chloride Ionic Liquids. Physical Chemistry Chemical Physics.* doi:10.1039/d0cp01686a.

11- Nasirpour, N., Mohammadpourfard, M., & Zeinali Heris, S. (2020). *Ionic liquids: promising compounds for sustainable chemical*

processes and applications. Chemical Engineering Research and Design. doi:10.1016/j.cherd.2020.06.006.